Potassium modified ZSM-5 catalysts for methyl acrylate formation from methyl lactate: the impact of the intrinsic properties on their stability and selectivity

Ekaterina V. Makshina†, Judit Canadell‡, Jan van Krieken‡, and Bert F. Sels*†*

† Centre for Sustainable Catalysis and Engineering, KU Leuven, Celestijnenlaan 200F, 3001 Heverlee, Belgium

‡ Central R&D, Corbion, Arkelsedijk 46, 4206 AC Gorinchem, The Netherlands

* E-mail: bert.sels@kuleuven.be (B.S.)

* E-mail: ekaterina.makshina@kuleuven.be (E.M.)

KEYWORDS: methyl lactate conversion, bio-based acrylates, zeolite catalyst, ion-exchange, potassium ZSM-5

ABSTRACT: Methyl lactate (ML) conversion to methyl acrylate is studied in the gaseous phase over ZSM-5 zeolite catalysts. High acrylate selectivity and catalyst service time were achieved using K-ZSM-5 catalyst with low content of Brønsted acid sites (below 1 μmol g^{-1}) and an overall K-to-Al atom ratio of unity. Feeding of ML in MeOH containing 5 to 25 vol.% of water improves the catalyst stability. As such, up to 80% acrylate yield at complete ML conversion, along with minor deactivation after days-on-stream and fully recoverable catalysis, are presented.

INTRODUCTION

Shortage and price fluctuations of oil-derived raw materials and the global environmental awareness lead to widespread efforts towards the development of alternative chemical processes utilizing renewable, bio-based resources. As market introduction of new 'green' building blocks is challenging, current initiatives concentrate largely on the discovery of novel sustainable and economically feasible synthesis routes for drop-in chemicals.[1–7] Among the list of industrial relevant chemicals, acrylic acid (AA) and its esters gain great attention due to its market size, price

and growth perspectives, while its synthesis from biomass is strongly motivated by the high functionality of the molecule, and potentially high atom economy to form acrylates from carbohydrates.[8,9] Catalytic dehydration of lactic acid (LA), quantitatively derived from carbohydrate through fermentation, is an attractive target reaction to produce bio-based AA (Scheme 1).[8,10]

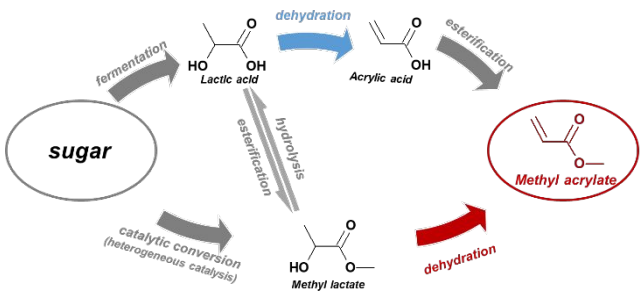

Scheme 1. Overview of the different processes for production of bio-acrylic acid and esters from sugars via lactic intermediates. The blue colored route indicates the most studied pathway in literature; the red colored route indicates the pathway of this work.

Its methyl ester (MA) is also an important monomer used for leather finishing, coatings, adhesives, plastics and textile fibers with worldwide annual production of 200 *k*tons, and currently prepared by AA esterification. Direct MA nitrilation for instance has high potential to produce bio-

acrylonitrile for the carbon fiber market.[11] MA manufacturing through dehydration of methyl lactate (ML) may provide an alternative sustainable production.

Though less studied than LA to AA, ML to MA may have several advantages. *i*) Inspection of the thermodynamics reveals a more favorable ML dehydration (discussion about thermodynamics is available in SI). *ii*) Given ML is formed in the industrial purification of LA after sugar fermentation, mature technology is available. *iii*) Recent research has demonstrated promising formation of ML from sugars and cellulose in methanol using homogeneous or heterogeneous catalysts.[12–18] *iv*) In contrast to LA, use of ML enables the utilization of highly concentrated feedstock without issues of self-oligomerization in the feedstock solution. *v*) ML has a lower boiling point and heat of evaporation (Table S1). And finally, *vi*) ML is more stable and less prone to thermal decomposition via decarbox(n)ylation pathways into acetaldehyde (AcH) and carbon oxides compared to LA. Since these side-reactions are thermodynamically more favorable, design of proper catalysis is of utmost importance to reach high MA yield.

Similar to LA conversion, bulk[19–23] and supported[24–26] phosphates and sulfates[19,27] as well as NaY and NaX zeolites[28–33] were also suggested as catalyst. The best results with selectivity reaching 80% were reported over 13X zeolite,[28,29] $Ca_3(PO_4)_2$-$Ca_2P_2O_7$[21] and sulfate catalyst

$KH_2PO_4/Na_2HPO_4/CuSO_4/CaSO_4$[27] (Table S2). However multicomponent systems are difficult to reproduce though proper balance between components (responsible for required surface acid and basic sites density) is a key for excellent catalytic performace in LA nd ML dehydration. Next to this the study of the catalytic stability at longer time on streams is often ignored or instability was observed. Moreover, in most of the studies water containing feedstock of ML was used leading to AA formation, while MA yield was low.

This work shows a high catalytic stability and high MA yield by converting ML over K-ZSM-5. To reach the excellent and stable catalytic performance, it will be demonstrated that the use of K-ZSM-5 with extremely low structural Brønsted acidity, preferentially below 1 μmol g^{-1}, and a K-to-Al atomic ratio close to but not exceeding unity is required. Besides, composition of the diluent matters a lot for the catalytic stability. Preferably, ML is fed as a dilution in methanol containing 5 to 25 wt.% of water, to obtain service lifetimes over several days.

EXPERIMENTAL SECTION

Catalysts synthesis

Among all tested zeolites used in the screening work, KL(3) (KL, supplied by Uetikon), NaMOR(7) and NaMOR(10) (CBV-10A, supplied by Zeolyst, and TSZ-640NAA, supplied by

Toyo Soda), NaZSM-5(12) and NaZSM-5(27) (SN27 and SN55 respectively, supplied by Alsi-Penta), KFER(10) (TSZ-740KOA, supplied by Toyo Soda) were used as received. All other zeolites, namely NaX(1.0) (UOP-13X, supplied by UOP), NaY(2.5) (CBV-100, supplied by Zeolyst), ZSM-11(22) (Na-ZSM-11-2, supplied by Bonding Chemical), FER(28) (CP914, supplied by Zeolyst), were subjected to ion-exchange using $NaNO_3$ using the procedure 1 describe below. Chabazite (KCHA) catalyst was synthesized via recrystallization of a commercial HY zeolite (CBV-100) according to procedure reported elsewhere[34] and was subjected to ion-exchange with KNO_3 using procedure 1 descried below.

Table S3 summarize the experimental details used for the synthesis of ZSM-5 based catalysts and labeling used in the main text of the manuscript. NaZSM-5 and NH_4ZSM-5 with Si/Al atomic ratio of 12 (SN27 and SM27 respectively, supplied by Alsi-Penta) were used as starting zeolite powders.

Ion-exchange procedure 1 – single exchange procedure. Air-dry zeolite powder was stirred in an aqueous solution of MNO_3 (where M is Na or K) for 20 h using the liquid to solid ratio (LSR) as specified in the Table S3 (e.g. in a typical synthesis, 400 ml of 1 M $NaNO_3$ or KNO_3 solution was used for 10 g of zeolite). The obtained material was filtered and washed with Millipore water

in order to remove the remaining salts using the LSR as specified in the Table S3 (e.g. in a typical synthesis, 600 ml of Millipore water for 10 g of zeolite was added during the washing step). The sample was dried at 60 ˚C overnight and calcined in a muffle oven at 550˚C for 4 h in static air with the ramp of 3˚C/min.

Ion-exchange procedure 2 – exchange procedure at elevated temperature according to procedure reported by Yan et al.[35] Air-dry zeolite powder was stirred in an aqueous solution of 0.5 M MNO_3 for 1h at 80˚C using LSR of 20. Afterwards, the zeolite was filtered, washed with Millipore water, and dried at 60˚C overnight. This procedure was repeated three times without intermediate calcination step. Finally the material was calcined in a muffle oven at 500˚C for 3 h in static air with the ramp of 3˚C/min.

Ion-exchange procedure 3 – double exchange procedure. In this case air-dry zeolite powder was stirred in an aqueous solution of 1M KNO_3 for 6 h (using LSR of 40), filtered and washed, and dried at 60˚C overnight. The ion-exchange procedure was repeated without an intermediate calcination step. During the synthesis of KZ(12)-2ex(n+h) a mixture of potassium nitrate and potassium hydroxide was used during the second exchange step, while the first exchange step was done only with the nitrate salt.

Ion-exchange procedure 4 – use of additives during the washing step. Catalysts washed with KOH, NaOH and NH_4OH were prepared according to the ion-exchange procedures 1 or 3. After the removal of mother liquor, firstly a portion of Millipore water was added (LSR of 20, e.g. in a typical synthesis; 200 ml of Millipore water was used for 10 g of zeolite) followed by a portion of MOH solution, where M is Na, K or NH_4, using LSR of 40 (e.g. in typical synthesis; 400 ml of 10 mM MOH solution was used for 10 g of zeolite). In the case of double exchange method (procedure 3), washing with additives was applied only after the second exchange.

Catalytic testing

98% methyl (S) lactate (Purasolv ML/CRG) was used as substrate. Methanol, water or mixture of water with methanol were used as solvents for ML dilution. The catalytic conversion of methyl lactate to methyl acrylate was carried out in a fixed bed continuous downstream flow reactor. The reaction was performed at 320-360 ˚C and atmospheric pressure. Typically, 1 g of catalyst, pelletized to a 0.25–0.5 mm fraction, was used. In order to avoid thermal decomposition of substrates and products in the reactor, the quartz reactor tube was filled with quartz wool below the catalyst bed and with glass beads above the catalyst bed. Blank tests at reaction temperature without catalyst have been conducted and no significant level of conversion was detected during

these tests. Methyl lactate solution was pumped in the system (with rate of 0.015 ml/min for standard tests conditions) using an HPLC pump (Waters 515) and mixed with N_2 (flow rate of 10 ml/min for standard reaction conditions) to ensure complete evaporation.

Products were analyzed by on-line gas chromatography (GC) equipped with a CPWAX 52CB column (20 m x 0,25 mm x 0,20 μm) and an FID detector. Carbon balance was calculated as total carbon amount in the analyzed products, divided by the total amount of carbons fed. Total conversion (TC, C% based on ML fed) was calculated according to the equation (1):

$$TC = \frac{n_{ML(fed)} - n_{ML(left)}}{n_{ML(fed)}} \cdot 100. \quad (1)$$

Yields (Y_i) of the products were calculated according to the equation (2):

$$Y_i = \frac{n_{x_i}}{n_{ML(fed)}} \cdot 100. \quad (2)$$

Selectivity (S) toward i-product was calculated as follows (equation (3)):

$$S_i = \frac{Y_i}{TC} \cdot 100, \quad (3)$$

where n_{x_i} is an amount of C moles of i-product.

Characterization techniques

The specific surface areas and porosity of the catalysts were determined by nitrogen adsorption at 77 K on a Micromeritics Tristar 3000 instrument. All samples were degassed under nitrogen

flow at 673 K for 6 h before the measurements. Micropore volume was determined from t-plot using standard method proposed by Harkins and Jura. Total pore volume was estimated from adsorption branch of isotherm as total volume adsorbed at p/p0 = 0.9. Surface area was calculated using Rouquerol method.[36]

IR experiments were performed on a Nicolet 6700 spectrometer equipped with a DTGS detector (128 scans; resolution of 2 cm^{-1}). Self-supporting wafers were pretreated in vacuum at 400˚C for 1 h (5 ˚C/min) before measurements. Acidity of the catalysts was analyzed using pyridine as probe. After pretreatment at 400 K, the samples were saturated with about 28 mbar of pyridine vapor at 50˚C for 20 min. The evacuated samples containing the adsorbed pyridine were heated up to 150˚C, kept for 20 min and then IR spectra were recorded. The integrated molar extinction coefficients used in acidity quantification were 1.67 $cm{\cdot}micromol^{-1}$ and 2.22 $cm{\cdot}micromol^{-1}$ for the 1545 cm^{-1} band characteristic for Brønsted acid site and 1455 cm^{-1} band characteristic for Lewis acid site respectively (according to the data reported in [37]).

Elemental composition was measured by ICP-OES analysis. 100 mg of dry powder was mixed with 500 mg of lithium borate ($LiBO_3$). Powder mixture was then transferred into graphite melting pot and placed in the muffle oven at 1000˚C for 10 min. Obtained melt was immediately transferred

to the beaker containing 50 ml 0.42M HNO_3 and kept under vigorous stirring for another 10 min. Next, probes were diluted 1/10 with 3wt% HNO_3 aqueous solution and measured by ICP OES (Varian 720-ES). Standard clay reference samples with known composition were taken as standards for calibration curves.

The ^{1}H-^{13}C cross polarization NMR experiments (CPMAS) were performed on a Bruker Ultrashield 300 MHz spectrometer (static magnetic field of 7.05T) with 4 mm H/X MAS probe at room temperature with a rotor spinning rate of 14 kHz. The ^{1}H-^{13}C CPMAS NMR spectra were recorded using 78 kHz RF field on ^{13}C, a RAMPed pulse on 1H (100–70%) for the contact time, 16384 scans, recycle delay of 2 s, ^{1}H SPINAL-64 decoupling, 29 and a contact time of 5 ms. The ^{13}C chemical shifts are referenced to TMS. The amount of sample used was ca. 90 mg.

Coke content on the spent catalysts was determined by thermal gravimetric analysis (TGA) using TGA Q500 (TA Instruments) equipped with an automatic sampler. Oxidative decomposition of carbon containing deposit was performed in a temperature-programmed regime under oxygen atmosphere (10% O_2 in N_2) with ramp of 5 $^{\circ}C \cdot min^{-1}$ to 600°C. The amount of soft and hard coke was calculated based on the weight loss in the range of 200-350°C and 350-500°C, respectively.

RESULTS AND DISCUSSION

Zeolites with various structural properties (topology) were selected in order to evaluate the effect of pores architecture on their catalytic performance in acrylates formation. Several important parameters were taken into account: pore size (8, 10 and 12 MR, where MR is membered ring windows which determine the pore size), dimensionality (1D, 2D and 3D), presence of cavities and their size, and also Si/Al ratio. Our broad exploration shows the highest MA yield and most stable catalysis for K-ZSM-5 with a high Si to Al ratio of 12 (Table S4). Clearly, use of other zeolites gave substantially lower MA yields and fast catalyst deactivation, issues that have been recognized also by others for LA conversion.[35,38]

Notably, whereas one literature reports high MA selectivity in presence of NaX,[28,29] we identified 2-methoxy methyl propionate (MMP) as the dominant product and not MA. Besides, in contrast to the report, the catalysis was only shortly stable - few hours which is in line with other reports [38] (Fig. S2). Moreover, our observed product distribution is in line with data reported in a patent elsewhere,[39] and therefore one can conclude high and stable MA selectivity over NaX that the early claimed in [28,29] cannot be confirmed.

K-ZSM-5 zeolite has not been studied so far in detail for the gas phase ML to MA dehydration. Therefore, a series of K exchanged ZSM-5 samples, with varying degree of exchange, was prepared to identify catalytic parameters that affect MA selectivity and catalyst stability. Different single- and double ion-exchange (with KNO_3) and washing procedures were screened using commercial Na-ZSM-5 with Si to Al atomic ratio of 12, *viz.* NaZ(12).

The synthesis variations provide numerous K-ZSM-5 catalysts with *i*) different K exchange fractions (between 0 and 1), *e.g.*, by varying K concentration in the exchange solution, *ii*) varying contents of BA acidity (between 0 and 6 μmol g^{-1}), *e.g.*, by washing with NH_4OH to deliberately reintroduce H^+, and *iii*) an excess of K (between 1 and 1.1 K to Al atomic ratio) *e.g.*, by decreasing amount of water during washing step or washing with a diluted KOH solution. The details of the preparations and catalyst properties are available in Table S3 and S5, respectively.

Representative time-on-stream (TOS) profiles of some of the tested catalysts are illustrated and compared in Fig. 1a (evolution of conversion and acetaldehyde yield in time are presented in Fig. S3). All curves show a general evolution: a low MA yield in the first hours (the initial period), followed by a plateauing high total acrylates (MA and AA) yield (the stable period), for which the yield decline is less than 2%, before MA yield drops substantially with time-on-stream

(deactivation period). Replacing Na by K in ZSM-5 clearly reduces the initial activation period and increases both the catalyst stability and selectivity towards acrylate formation (see Fig. 1b). There is an almost linear increase of acrylate selectivity, *viz.* from 60 to 80%, with the K fraction, which is largely due to lowering of AcH formation. Striking is the exponential beneficial effect of K on the stability of the catalytic performance. Dehydration catalysis with Na-ZSM-5 is only stable for a few hours, alike many other reported catalyst types, whereas introducing K in ZSM-5 stabilizes the catalysis for more than 30 hours on stream without significant drop in ML conversion and MA yield. While this K effect on MA selectivity may at first sight resemble that observed for LA to AA,[40] such kind of correlations affecting the catalytic stability of ML to MA reaction has never been reported.

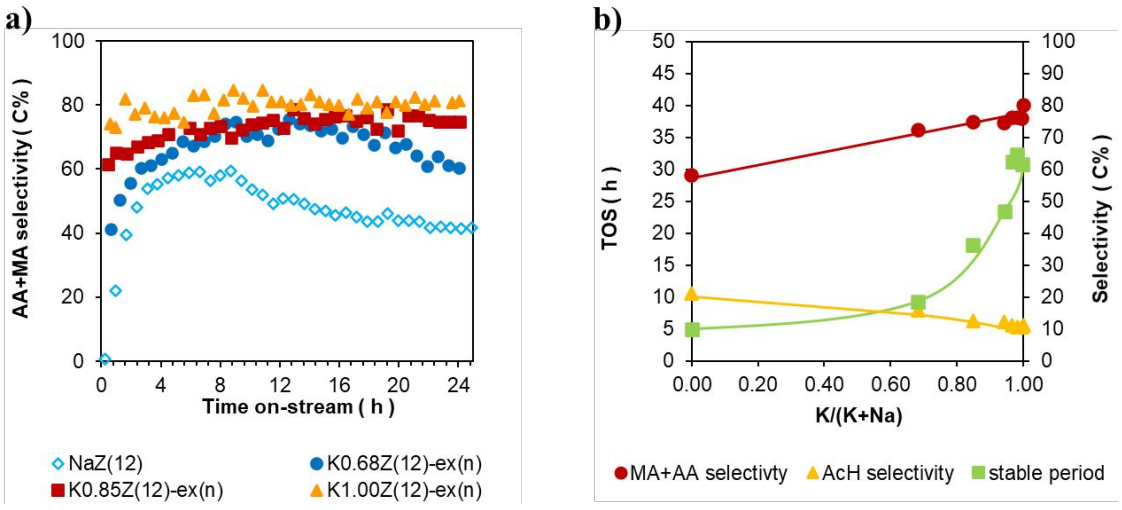

Figure 1. (a) Time-on-stream behavior (TOS), and (b) the impact of K exchange degree in ZSM-5 on stability and selectivity, tested in ML conversion in following conditions: 340˚C, 35 wt.% ML in MeOH, and 5.6 mol.% of ML in total gas stream (0.5 h^{-1} liquid hourly space velocity - LHSV). The lines are guides to the eye.

Brønsted acidity and coke characteristics of the different starting and spent Na- and K-ZSM-5 catalysts, respectively, were determined and compared in order to elucidate the peculiar K effect (Fig. 2). Pyridine probe FTIR, and not the more commonly used NH_3 TPD method in related catalytic studies,[35,40] was deliberately used to monitor the low contents of residual Brønsted acidity (on fresh samples). Replacement of Na by K cations results in a slight shift of the band of pyridine adsorbed on Lewis acid sites from 1442 cm^{-1} to 1438 cm^{-1}, which is related to the weaker interaction of acid sites with pyridine molecule (Fig. S4).[41] This shift makes it impossible to clearly distinguish the amount of pyridine adsorbed Lewis acid sites and OH groups, and thus also their proper quantification by band deconvolution. Hence, quantitative correlation of catalytic activity with the number of Lewis acid sites is not made in this study. The drop of Lewis acidity (from the combined band of Lewis acid and OH-groups) of K-containing zeolites compared to Na-forms is

described in literature[42,43] and explained by a decrease in acid strength (Fig. 2a). Note that FTIR measurements were performed at 150˚C, excluding some very weak acid sites. K exchange on the parent Na-ZSM-5 causes a strong decrease of Brønsted acid sites content, *viz.* from 6 to essentially 0 µmol g^{-1} for a K fraction varying from zero to unity (Fig. 2a). Therefore, care has to be taken to explain catalytic effects by only presence of (more basic) K ions, while Brønsted acidity also varies significantly, a point that has been ignored so far in explaining the 'K effect' in LA to AA studies.

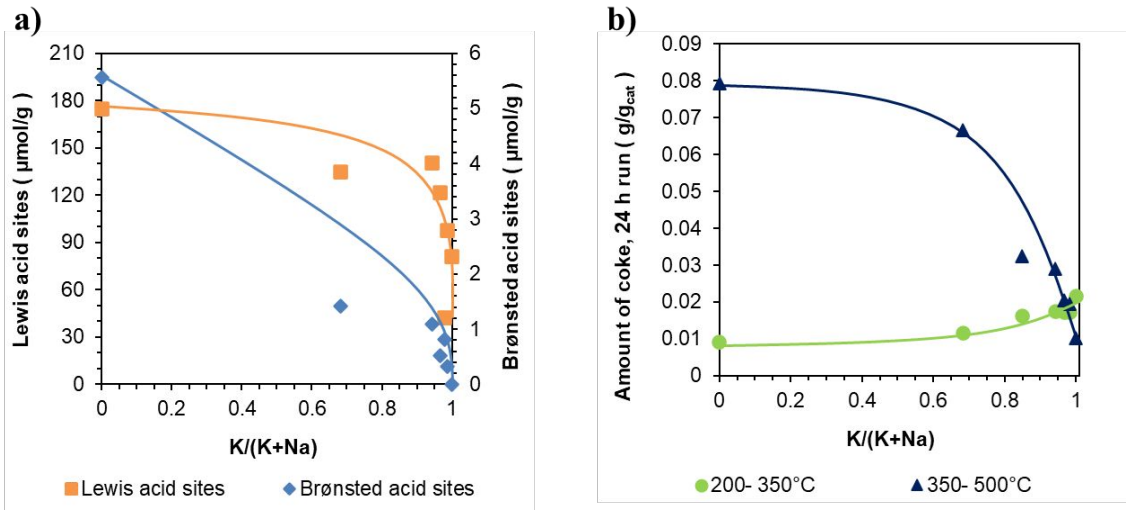

Figure 2. Amount of Lewis and Brønsted acid sites (a) and amount of coke accumulated during 24h runs (b) vs. potassium content. The lines are guides to the eye.

Catalyst deactivation was investigated through a coke study. The amount and type of coke were measured with TGA under air atmosphere using spent catalysts. Two distinct coke types were identified on the spent catalysts: one between 200˚C and 350˚C, and another one above 350˚C (Fig. S5 a-b). Low temperature coke (further denoted as "soft coke", decomposition temperature in the range of 200-350˚C) is the dominant type of coke with the degree of K exchange higher than 0.97, while high temperature coke (further denoted as "hard coke", decomposition temperature above 350˚C) is mostly present for lower K contents (Fig. 2b).

Solid state ^{13}C MAS NMR and FT-IR were used to identify the major functional groups in the coke structure (Fig. S6-S7). According to the carbon chemical shifts in ^{13}C MAS NMR (see Fig. S6), the low temperature (soft) coke features carboxylic/ester group (with a chemical shift at 175 ppm), likely due to lactate (oligomer) species, whereas the high temperature (hard) coke clearly shows unsaturation features, represented by the 130 ppm chemical shift. FTIR measurements support the NMR coke analysis (Fig. S7). It further indicates absence of aromatics in the hard coke due to lack of the diagnostic aromatic C-H vibration above 3000 cm^{-1}. The presence of the band at 1740 cm^{-1} attributed to C=O group of lactates[44] confirms the lactyl origin of the soft coke species.

In order to decouple the effect of Lewis acidity (related to presence of more basic K cations sites) and removal of Brønsted acidity during ion-exchange, Brønsted acid sites were deliberately introduced into K-ZSM-5 during the synthesis, thus leading to series of Na-free, but H-containing K-ZSM-5. The performance of different Na- and K-ZSM-5 catalysts is displayed in Fig. 3a in function of acid content (time-on-stream curves, Fig. S8). Irrespective of the cation type Na or K, both the stability and MA selectivity decreases substantially with increasing amount of Brønsted acid sites, even though the Brønsted acid sites contents under study are in the low μmoles per gram range. In other words, the absence of zeolite structure-related protons appears essential to reach performant (selective and stable) ML dehydration catalysis. AcH formation clearly increases with acidity (Fig. 3b), with a small difference between Na and K-ZSM-5. K-ZSM-5 is thus limiting somewhat acetaldehyde formation in favor of acrylates, but the major reason of high MA selectivity and catalyst stability is the absence of zeolitic Brønsted acidity.

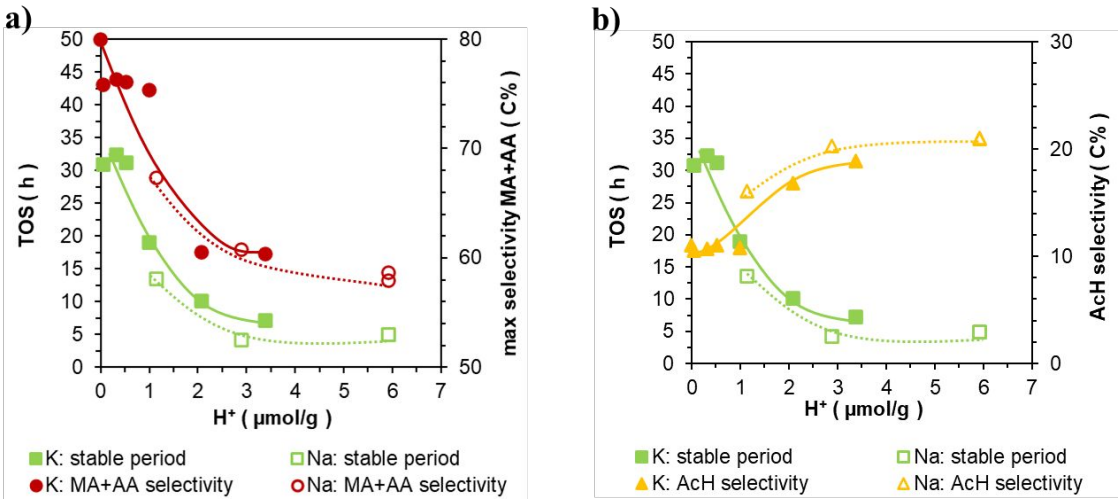

Figure 3. Effect of residual Brønsted acid on stability and acrylates selectivity (a) and acetaldehyde selectivity (b). Reaction conditions: 340˚C, 35 wt.% ML in MeOH, 5.6 mol.% of ML in total gas stream corresponding to 0.5 h^{-1} LHSV. The lines are guides to the eye

The content and type of coke on the spent catalysts is strongly related to Brønsted acidity present in the fresh catalyst (Fig. 4a), but also to the cation type. There is more hard coke formed on Na-ZSM-5, possessing stronger Lewis acidity, up to 9 wt.%, for the same amount of Brønsted acid sites, while the amount of soft coke is lower, 1 to 2 wt.%, and similar for Na and K-ZSM-5 samples. Increasing amounts of Brønsted acids favors hard coke formation but lowers the content of soft coke. Bringing together the acidity and coke results reveals that the most stable and selective ZSM-5 catalyst avoids hard coke formation (Fig. 4b). These catalysts are capable of converting ML into

acrylates at 80% selectivity and full ML conversion, and that for more than 30 h on stream before the appearance of slow deactivation. One step further from here, Figure 5 (and Figure S9), demonstrate full and multiple recovery of the catalysis by classic air calcination of the spent catalyst bed (at 450˚C), signifying the long term production of MA.

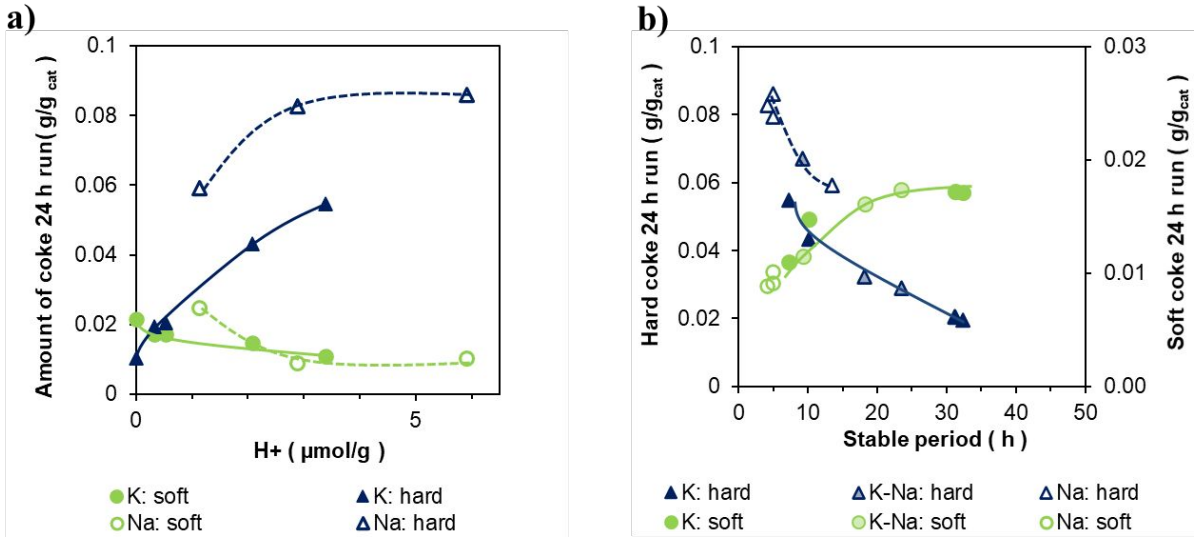

Figure 4. Coke content (a) of the Na- (open symbols) and K-ZSM-5(12) materials (closed symbols) with different content of Brønsted acid sites in ML conversion; (b) relationship between hard and soft coke content on the spent catalysts and the catalytic stability on stream for 3 series of catalysts with only Na, only K and mixed Na-K with different H^+-content (coke content analyzed after 24h run). The lines are guides to the eye

Rather than to solve catalyst stability by regeneration avoiding hard coke formation is likely a more sustainable strategy, and therefore understanding this coke formation is imperative to improve the catalysis stability. Although strong Brønsted acid sites in ZSM-5 are well-known to convert methanol into olefins and aromatics (in the MTH process) at 340˚C, we verified that methanol itself is not the origin of the hard coke in the conversion of ML to MA. To substantiate this point, two K-ZSM-5 catalysts with low (0.3 μmol g^{-1}) and high proton content (3.4 μmol g^{-1}) were contacted with pure MeOH at similar reaction conditions (Fig. S10-S11). Given no formation of high temperature coke after 24 h on stream, MeOH is not the main cause of hard coking and catalyst deactivation. On the contrary, the presence of MeOH is mandatory to reach the best stability of the catalytic results. Indeed, when pure ML (at the same partial pressure) is fed into the reactor over K-ZSM-5, very poor catalysis (showing fast deactivation and lower acrylate selectivity) is obtained (Fig. S12). Possible transformation of MA, prone to polymerization, into hard coke deposit was also excluded since no significant hard coke formation was noticed after contacting MA/MeOH feed mixtures over the catalyst with high Brønsted acidity (Fig. S13). Thus ML itself or the formed acetaldehyde, perhaps through condensation, is the most probable origin of hard coke deposits (*vide infra*).

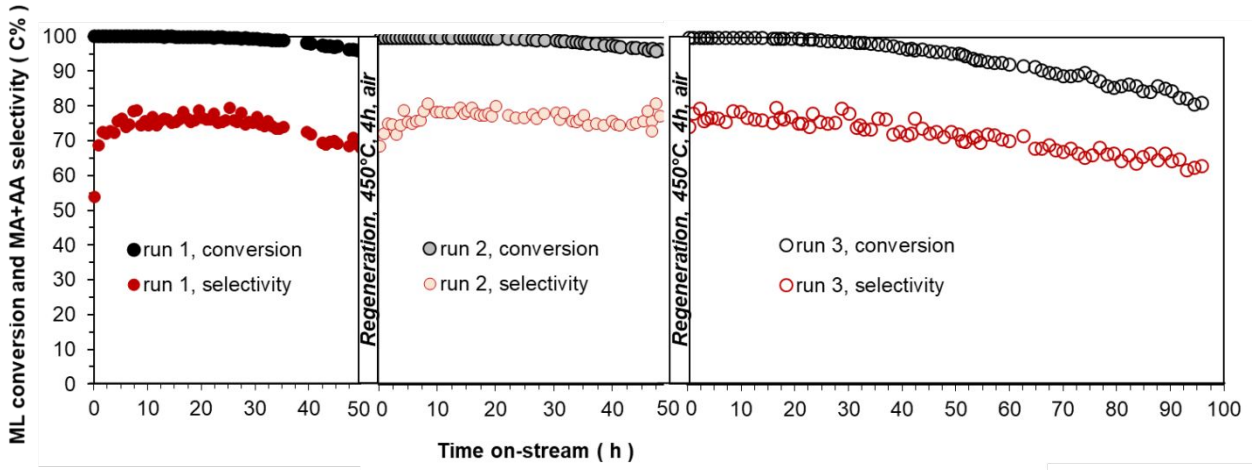

Figure 5. Time-on-stream (TOS) behavior of proton-free K-ZSM-5 catalyst with 2 regeneration steps (calcination in air at 450˚C, 4 h) after 50h run (reaction conditions: 340˚C, liquid feedstock: 35 wt.% ML/MeOH, 5.6 mol.% of ML in total gas stream). Fig. S9 shows a full overlap of run 1 and run 3 (fresh catalyst and catalyst after 2 regeneration cycles)

In addition to the effect of Brønsted acid sites and choice of cation on the coke, further improvement of the catalyst service time was achieved by water addition to the liquid ML/MeOH feed. The influence of the water content on the catalyst life time and acrylate selectivity is displayed in Figure 6. The addition of small amounts of water, in the range of 5 to 25 wt.%, more than doubled the service time, without affecting the methyl acrylate selectivity. For instance, stable 71% MA and 7% AA yield were obtained during a period of 65 hours, followed by minor

deactivation. The selectivity of MA within the acrylate fraction thus only slightly decreased from 96 to 92% for the required water content.

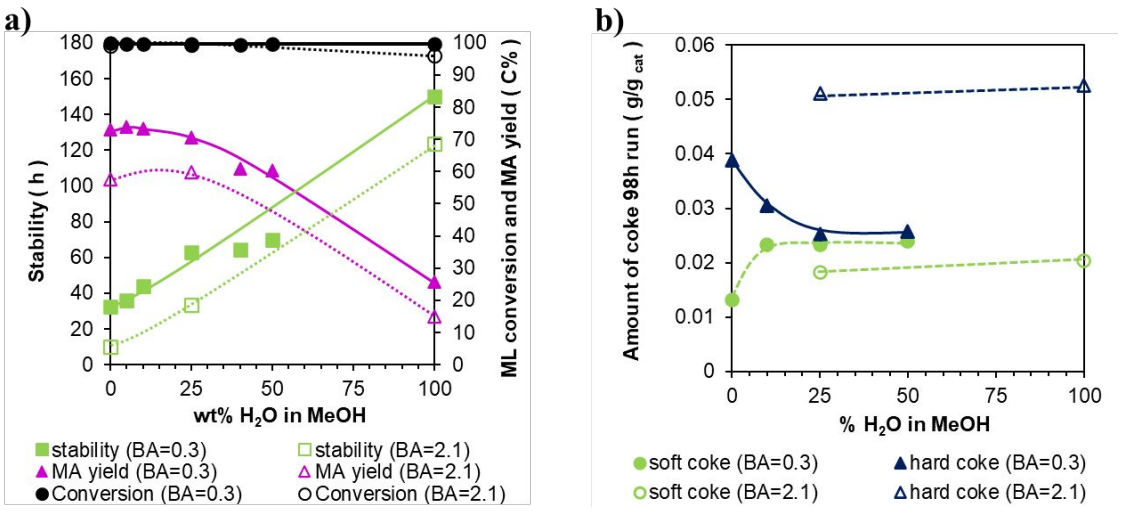

Figure 6. Water effect on the catalytic performance (a) and coke content (b) of K-ZSM-5 with low (0.3 μmol g^{-1}) and high (2.1 μmol g^{-1}) Brønsted acidity (BA) content in ML conversion. C conditions: 340˚C, liquid feedstock: 35 wt.% ML / X wt% H_2O in MeOH, 5.6 mol.% of ML in total gas stream. The lines are guides to the eye.

TG analysis of the spent catalysts showed a decrease of the high temperature (hard) coke amount with the increase of water content in the ML feed in that range, again indicating that inhibition of hard coke formation serves a longer catalyst lifetime. Increasing the water content above 25 wt.% leads to a sharp drop in MA selectivity despite of the catalyst lifetime increase. AcH formation is

barely impacted by the MeOH to water replacement (slight increase in AcH selectivity from 11% for ML/MeOH feedstock to 13% for ML/H_2O feedstock was observed), indicating that AcH is not the main source of hard coke formation. The stabilizing effect of water due to inhibiting hard coke formation is also observed for ZSM-5 catalysts with the higher Brønsted acidity content, but the stability and catalytic performance never exceeded that of the essentially proton-free ZSM-5 catalysts (Fig. 6).

ML catalysis is thus very sensitive, through coke formation, to the presence of structural zeolitic protons in the K-ZSM-5 catalyst. This implicates that the catalyst synthesis should be carried out with great care. Indeed, many synthesis steps may leave or reintroduce low contents of Brønsted acidity, which are detrimental for the catalysis stability and acrylate selectivity. For instance, exchanging K directly on H-ZSM-5 or NH_4-ZSM-5 parent zeolites should be avoided because such procedures result in substantial amounts of residual protons. Excessive washing of catalysts after the exchange process may also reintroduces protons. For instance, the resulting 1.0 μmol H^+ g^{-1} proton density and the drop in stability from ca. 33 h to 19 h was clearly observed when the volume amount of water during the washing step was increased to more than 3 times (compared to the standard procedure here).

Although extensive washing is undesirable, sufficient washing to avoid K excess is also necessary. Figure 7 (and Fig. S14) plots the catalytic performance (stability and selectivity) of K-rich ZSM-5 samples (while keeping the content of BA below 1 μmol g^{-1} by applying different washing procedures; details in SI), against the K to Al atomic ratio. The strong drop in catalytic stability, once the K to Al ratio exceeds unity, is apparent. Coke investigation of the spent K-rich catalysts (after 24 hours) reveals that hard coke is barely formed, but the soft coke content substantially increased with excess of K. Although no significant drop in micropore volume of the spent catalyst was observed, likely, the excess of K induces the formation of lactic oligomers and limit the accessibility of active sites.

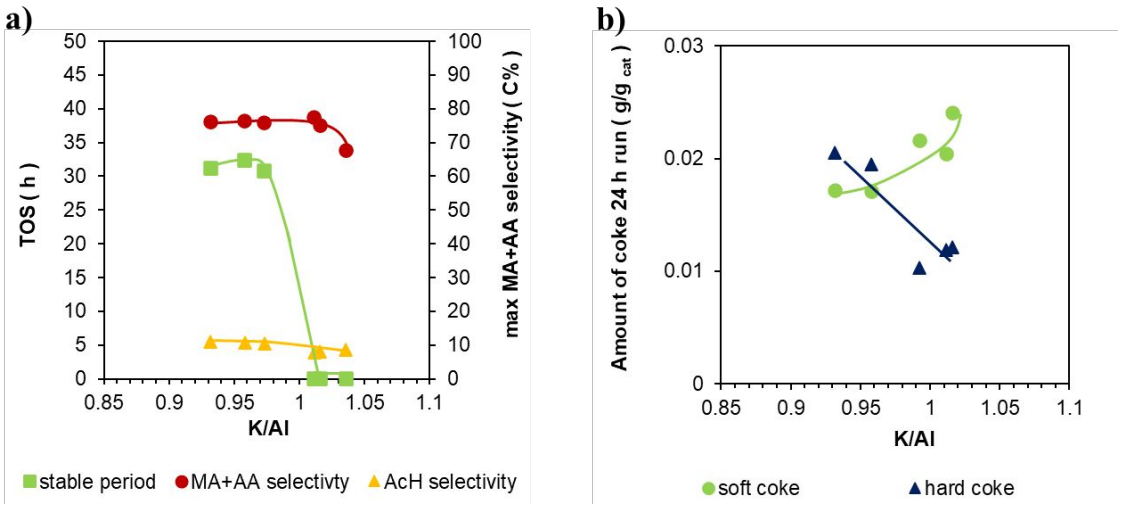

Figure 7. Catalytic performance (a) and coke content (b) of the K-rich K-ZSM-5(12) materials with varying K/Al ratio (K/(K+Na) > 0.97) but similar Brønsted acidity (<1 μmol g^{-1}) in ML

conversion. Reaction conditions: 340˚C, 35 wt.% ML in MeOH, 5.6 mol.% of ML in total gas stream (0.5 h^{-1} LHSV).

Recent mechanistic studies of LA and ML dehydration suggest that Lewis acid sites are responsible for the dehydration activity, whereas Brønsted acidity lower MA selectivity due to acetaldehyde and coke formation.[45–47] This work shows that the structure-related acid sites, even at very low concentration, contribute largely, and they are even more important to consider for catalyst instability than the *in situ* Brønsted acid sites that are formed during the catalytic cycle, as suggested earlier by Murphy *et al.*[45–47] It is generally accepted that the dehydration mechanism starts with an interaction of methyl lactate with the cation (here, K or Na), forming an adsorbed methoxy species and lactate salt (Scheme 2). Dehydration, presumably involving the Lewis acid site, leads to K (or Na) acrylate and one water molecule. Recent spectroscopic studies suggest the formation of acrylic acid as primary product while esterification leading to acrylic ester is a separate consecutive step in the reaction pathway.[48] At the same time, water released during the reaction (especially at high conversion) or present in the system as diluent favors the formation of

in situ Brønsted acid site via hydrolysis of the methoxy species, while K (or Na) ions are linked to lactate moiety.

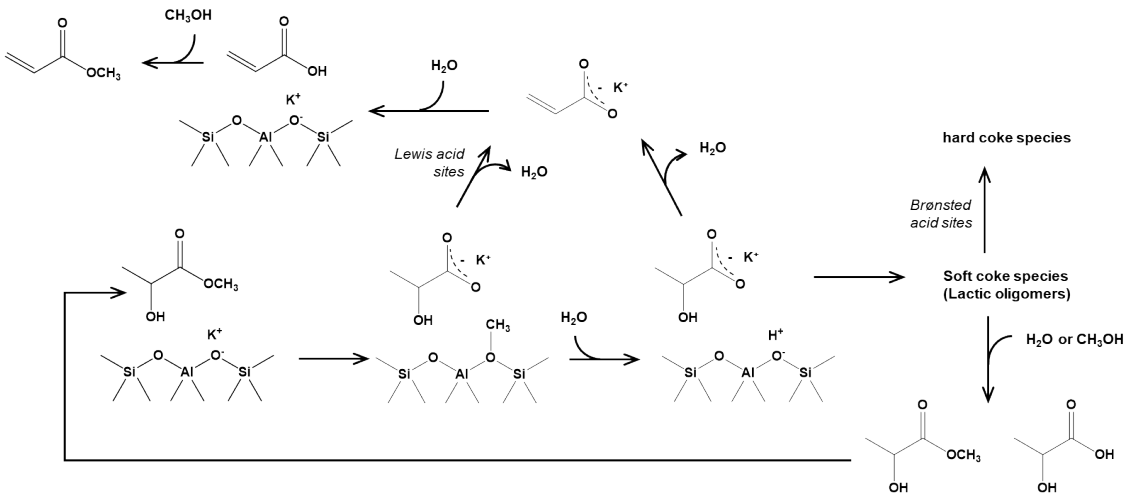

Scheme 2. Tentative scheme of the process including formation of acrylates, coke formation, recuperation of the substrate through partial decomposition of soft coke

Proton containing zeolites are reported to form lactic oligomers.[49] Hence it is reasonable to assume that the high surface residence time of such oligomers enables further chemical transformation, favoring degradation pathways through ring-formed oligomers as a result of intramolecular esterification within the temperature range of 300-400˚C.[50,51] We assume that such degradation products, together with the lactyl oligomer precursors, all containing C=O ester

moieties, are reflecting the soft cokes species, as observed in TGA and analyzed with ^{13}C MAS NMR and FT-IR.

Formation of hard coke most probably involves typical carbocation and hydride shift chemistry (alkylation, carbon-carbon skeleton rearrangements, etc.) during catalytic fragmentation of oligomer chains catalyzed mainly by Brønsted acid sites, with some contribution as well from cations with strong Lewis acidity given the fact that more hard coke is formed over Na-ZSM-5 catalysts compared to K-ZMS-5 catalysts independently of the proton density. Our results indicate that the (overlooked) Brønsted acid sites play a dominant role in coke formation and fast deactivation and the *in-situ* formed ones plays secondary role given the improved stability of K-ZSM-5 when free of zeolitic protons (showing slow deactivation rate only at longer time-on-stream).

Mechanistically, high partial pressure of methanol or water is able to prevent the undesired fragmentation of oligomers that are transformed into hard coke by preferential hydrolysis (methanolysis) returning the lactyl oligomers to monomers, viz. lactic acid and methyl lactate (Scheme 2, bottom pathway). In absence of the reactive diluents such recuperation process is not efficient. Even at high conversion the amount of formed water is insufficient to prevent catalyst

deactivation. The suggested possibility to eliminate soft coke by adding additional amounts of water was verified (Fig. S15). The catalytic properties of partially deactivated spent catalyst containing both high and soft coke can be restored after in-situ steaming (done by replacing of ML/MeOH feed by water for 3h and back from water to ML/MeOH), indicating that water is most (in contrast to methanol) efficient to depolymerize via hydrolysis the adsorbed oligomers. This explains the observed higher stability of the catalyst and the higher selectivity when a certain amount of water is present in the reaction mixture next to methanol, while its balance will determine the fraction of ML within the sum of acrylates.

CONCLUSION

In summary, our results on ML to MA conversion over K-ZSM-5 comprehend the essential catalytic requirements. To get high acrylate selectivity (~80% at full conversion) and catalyst lifetime, absence of K excess (to avoid catalyst fouling), and extremely low structure-related Brønsted acidity (to reduce hard coke formation) are key. Presence of methanol and water in the ML feed further inhibits catalyst coking by reversing oligomerisation, the major cause of catalyst

instability. Service times of days are possible now, while prolonged catalyst usage is demonstrated by full catalyst recovery via coke burning.

ASSOCIATED CONTENT

Supporting Information. The Supporting Information is available free of charge on the ACS Publications website at DOI:

The supporting information contains: thermodynamic considerations; physical properties of substrates; overview of performance of selected catalysts reported in literature; details of synthesis and labeling of the catalysts; results of the screening of zeolites with different topologies; properties of prepared ZSM-5 zeolites; additional figures supporting results and discussion about impact of K exchange degree, proton density, regeneration tests, conversion of methanol, methyl acrylate, solvent free reaction, impact K/Al ratio and steaming experiment.

AUTHOR INFORMATION

Corresponding Author

* E-mail: bert.sels@kuleuven.be (B.S.)

* E-mail: ekaterina.makshina@kuleuven.be (E.M.)

ORCID

Bert Sels: https://orcid.org/0000-0001-9657-1710

Ekaterina Makshina: https://orcid.org/0000-0003-1461-5084

Notes

The authors declare no competing financial interest..

ACKNOWLEDGMENT

This work was funded by Corbion (Purac). Prof. Johan Martens and Dr. Eric Breynaert are acknowledged for the NMR measurements, and Elvira Vassilieva for the ICP-OES measurements. IOF KULeuven funding is greatly acknowledged.

REFERENCES

(1) Dusselier, M.; Van Wouwe, P.; Dewaele, A.; Jacobs, P. A.; Sels, B. F. Shape-Selective Zeolite Catalysis for Bioplastics Production. *Science* **2015**, *349* (6243), 78–80. https://doi.org/10.1126/science.aaa7169.

(2) Huber, G. W.; Iborra, S.; Corma, A. Synthesis of Transportation Fuels from Biomass: Chemistry, Catalysts, and Engineering. *Chem. Rev.* **2006**, *106* (9), 4044–4098. https://doi.org/10.1021/cr068360d.

(3) Corma, A.; Iborra, S.; Velty, A. Chemical Routes for the Transformation of Biomass into Chemicals. *Chem. Rev.* **2007**, *107* (6), 2411–2502. https://doi.org/10.1021/cr050989d.

(4) Wu, L.; Moteki, T.; Gokhale, A. A.; Flaherty, D. W.; Toste, F. D. Production of Fuels and Chemicals from Biomass: Condensation Reactions and Beyond. *Chem* **2016**, *1* (1), 32–58. https://doi.org/10.1016/j.chempr.2016.05.002.

(5) Pelckmans, M.; Vermandel, W.; Van Waes, F.; Moonen, K.; Sels, B. F. Low-Temperature Reductive Aminolysis of Carbohydrates to Diamines and Aminoalcohols by Heterogeneous Catalysis. *Angew. Chemie Int. Ed.* **2017**, *56* (46), 14540–14544. https://doi.org/10.1002/anie.201708216.

(6) Alonso, D. M.; Bond, J. Q.; Dumesic, J. A. Catalytic Conversion of Biomass to Biofuels. *Green Chem.* **2010**, *12* (9), 1493–1513. https://doi.org/10.1039/C004654J.

(7) Sharada, D.; Naresh, U.; Shiva, K. V.; Jeevan Kumar, R. Drop-in Plastics. In *Advanced Catalysis for Drop-in Chemicals*; Sudarsanam, P., Li, H., Eds.; Elsevier, 2022; pp 31–46. https://doi.org/10.1016/B978-0-12-823827-1.00007-9.

(8) Blanco, E.; Loridant, S.; Pinel, C. Valorization of Lactic Acid and Derivatives to Acrylic Acid Derivatives: Review of Mechanistic Studies. In *Reaction Pathways and Mechanisms in Thermocatalytic Biomass Conversion II: Homogeneously Catalyzed Transformations, Acrylics from Biomass, Theoretical Aspects, Lignin Valorization and Pyrolysis Pathways*; Schlaf, M., Zhang, Z. C., Eds.; Springer Singapore: Singapore, 2016; pp 39–62. https://doi.org/10.1007/978-981-287-769-7_3.

(9) Makshina, E. V.; Canadell, J.; van Krieken, J.; Peeters, E.; Dusselier, M.; Sels, B. F. Bio-Acrylates Production: Recent Catalytic Advances and Perspectives of the Use of Lactic Acid and Their Derivatives. *ChemCatChem* **2019**, *11*, 180–201. https://doi.org/10.1002/cctc.201801494.

(10) Dusselier, M.; Van Wouwe, P.; Dewaele, A.; Makshina, E.; Sels, B. F. Lactic Acid as a Platform Chemical in the Biobased Economy: The Role of Chemocatalysis. *Energy Environ. Sci.* **2013**, *6* (5), 1415. https://doi.org/10.1039/c3ee00069a.

(11) Karp, E. M.; Eaton, T. R.; Sànchez i Nogué, V.; Vorotnikov, V.; Biddy, M. J.; Tan, E. C. D.; Brandner, D. G.; Cywar, R. M.; Liu, R.; Manker, L. P.; Michener, W. E.; Gilhespy, M.; Skoufa, Z.; Watson, M. J.; Fruchey, O. S.; Vardon, D. R.; Gill, R. T.; Bratis, A. D.; Beckham, G. T. Renewable Acrylonitrile Production. *Science* **2017**, *358* (6368), 1307–1310. https://doi.org/10.1126/science.aan1059.

(12) de Clippel, F.; Dusselier, M.; Van Rompaey, R.; Vanelderen, P.; Dijkmans, J.; Makshina, E.; Giebeler, L.; Oswald, S.; Baron, G. V.; Denayer, J. F. M.; Pescarmona, P. P.; Jacobs, P. A.; Sels, B. F. Fast and Selective Sugar Conversion to Alkyl Lactate and Lactic Acid with Bifunctional Carbon–Silica Catalysts. *J. Am. Chem. Soc.* **2012**, *134* (24), 10089–10101. https://doi.org/10.1021/ja301678w.

(13) Holm, M. S.; Saravanamurugan, S.; Taarning, E. Conversion of Sugars to Lactic Acid Derivatives Using Heterogeneous Zeotype Catalysts. *Science* **2010**, *328* (5978), 602–605. https://doi.org/10.1126/science.1183990.

(14) West, R. M.; Holm, M. S.; Saravanamurugan, S.; Xiong, J.; Beversdorf, Z.; Taarning, E.; Christensen, C. H. Zeolite H-USY for the Production of Lactic Acid and Methyl Lactate from C3-Sugars. *J. Catal.* **2010**, *269* (1), 122–130. https://doi.org/10.1016/j.jcat.2009.10.023.

(15) Nemoto, K.; Hirano, Y.; Hirata, K.; Takahashi, T.; Tsuneki, H.; Tominaga, K.; Sato, K. Cooperative In-Sn Catalyst System for Efficient Methyl Lactate Synthesis from Biomass-Derived Sugars. *Appl. Catal. B Environ.* **2016**, *183*, 8–17. https://doi.org/10.1016/j.apcatb.2015.10.015.

(16) Tolborg, S.; Sádaba, I.; Osmundsen, C. M.; Fristrup, P.; Holm, M. S.; Taarning, E. Tin-Containing Silicates: Alkali Salts Improve Methyl Lactate Yield from Sugars. *ChemSusChem* **2015**, *8* (4), 613–617. https://doi.org/10.1002/cssc.201403057.

(17) Zhang, J.; Wang, L.; Wang, G.; Chen, F.; Zhu, J.; Wang, C.; Bian, C.; Pan, S.; Xiao, F.-S. Hierarchical Sn-Beta Zeolite Catalyst for the Conversion of Sugars to Alkyl Lactates. *ACS Sustain. Chem. Eng.* **2017**, *5* (4), 3123–3131. https://doi.org/10.1021/acssuschemeng.6b02881.

(18) Iglesias, J.; Moreno, J.; Morales, G.; Melero, J. A.; Juárez, P.; López-Granados, M.; Mariscal, R.; Martínez-Salazar, I. Sn–Al-USY for the Valorization of Glucose to Methyl Lactate: Switching from Hydrolytic to Retro-Aldol Activity by Alkaline Ion Exchange. *Green Chem.* **2019**, *21* (21), 5876–5885. https://doi.org/10.1039/C9GC02609F.

(19) Holmen, R. Production of Acrylates by Catalytic Dehydration of Lactic Acid and Alkyl Lactates. US 2,859,240, 1958.

(20) Hong, J. H.; Han, Y. H.; Kim, H. R.; Jang, J. S. Preparation of Calcium Phosphate Dehydration Catalyst for Preparation of Acrylic Acid and Acrylates from Lactates. KR 2012025888, 2012.

(21) Hong, J. H.; Lee, J.-M.; Kim, H.; Hwang, Y. K.; Chang, J.-S.; Halligudi, S. B.; Han, Y.-H. Efficient and Selective Conversion of Methyl Lactate to Acrylic Acid Using $Ca_3(PO_4)_2$-$Ca_2(P_2O_7)$ Composite Catalysts. *Appl. Catal. A Gen.* **2011**, *396* (1–2), 194–200. https://doi.org/10.1016/j.apcata.2011.02.015.

(22) Walkup, P. C.; Rohrmann, C. A.; Hallen, R. T.; Eakin, D. E. Production of Esters of Lactic Acid, Esters of Acrylic Acid, Lactic Acid, and Acrylic Acid. US 5,071,754, 1991.

(23) Walkup, P. C.; Rohrmann, C. A.; Hallen, R. T.; Eakin, D. E. Production of Esters of Lactic Acid, Esters of Acrylic Acid, Lactic Acid, and Acrylic Acid. US 5,252,473, 1993.

(24) Lee, J.-M.; Hwang, D.-W.; Hwang, Y. K.; Halligudi, S. B.; Chang, J.-S.; Han, Y.-H. Efficient Dehydration of Methyl Lactate to Acrylic Acid Using $Ca_3(PO_4)_2$-SiO_2 Catalyst. *Catal. Commun.* **2010**, *11* (15), 1176–1180. https://doi.org/10.1016/j.catcom.2010.06.013.

(25) Tan, T.; Mo, Z.; Liu, G.; Huang, H.; Han, C. Supported Composite Salt for Preparing Acrylic Acid and/or Acrylate by Dehydrating Lactic Acid or Lactate, Its Preparation Method and Application. CN102513137, 2012.

(26) Zhang, Z.; Qu, Y.; Wang, S.; Wang, J. Catalytic Performance and Characterization of Silica Supported Sodium Phosphates for the Dehydration of Methyl Lactate to Methyl Acrylate and Acrylic Acid. *Ind. Eng. Chem. Res.* **2009**, *48* (20), 9083–9089. https://doi.org/10.1021/ie900065a.

(27) Zhang, J.; Lin, J.; Xu, X.; Cen, P. Evaluation of Catalysts and Optimization of Reaction Conditions for the Dehydration of Methyl Lactate to Acrylates. *Chinese J. Chem. Eng.* **2008**, *16* (2), 263–269. https://doi.org/10.1016/S1004-9541(08)60073-7.

(28) Abe, T.; Hieda, S. Process for Preparing Unsaturated Carboxylic Acid or Ester Thereof. EP 0379691, 1990.

(29) Abe, T.; Hieda, S. Process for Preparing Unsaturated Carboxylic Acid or Ester Thereof. US 5,250,729, 1993.

(30) Bai, T.; Li, J.; Zuo, S.; Liu, J. Method for Preparation of Acrylate via Catalytic Dehydration of Lactate. CN 102001942, 2011.

(31) Bai, T.; Liu, J.; Li, B.; Zuo, S. Catalytic Dehydration of Lactate Esters to Acrylate Esters. *Gongye Cuihua* **2012**, *20* (2), 54–57. https://doi.org/10.3969/j.issn.1008-1143.2012.02.013.

(32) Ozmeral, C.; Glas, J. P.; Dasari, R.; Tanielyan, S.; Bhagat, R. D.; Kasireddy, M. R. Catalytic Dehydration of Lactic Acid and Lactic Acid Esters. WO 2012/033845, 2012.

(33) Shi, H. F.; Hu, Y. C.; Wang, Y.; Huang, H. KNaY-Zeolite Catalyzed Dehydration of Methyl Lactate. *Chinese Chem. Lett.* **2007**, *18* (4), 476–478. https://doi.org/10.1016/j.cclet.2007.01.043.

(34) Ridha, F. N.; Yang, Y.; Webley, P. A. Adsorption Characteristics of a Fully Exchanged Potassium Chabazite Zeolite Prepared from Decomposition of Zeolite Y. *icroporous Mesoporous Mater.* **2009**, *117* (1–2), 497–507. https://doi.org/10.1016/j.micromeso.2008.07.034.

(35) Yan, B.; Tao, L.-Z.; Mahmood, A.; Liang, Y.; Xu, B.-Q. Potassium-Ion-Exchanged Zeolites for Sustainable Production of Acrylic Acid by Gas-Phase Dehydration of Lactic Acid. *ACS Catal.* **2017**, *7*, 538–550. https://doi.org/10.1021/acscatal.6b01979.

(36) Rouquerol, F.; Rouquerol, J.; Sing, K. CHAPTER 11 - Adsorption by Clays, Pillared Layer Structures and Zeolites. In *Adsorption by Powders and Porous Solids*; Rouquerol, F., Rouquerol, J., Sing, K., Eds.; Academic Press: London, 1999; pp 355–399. https://doi.org/10.1016/B978-012598920-6/50012-9.

(37) Emeis, C. A. Determination of Integrated Molar Extinction Coefficients for Infrared Absorption Bands of Pyridine Adsorbed on Solid Acid Catalysts. *J. Catal.* **1993**, *141* (2), 347–354. https://doi.org/10.1006/jcat.1993.1145.

(38) Näfe, G.; Lopez-Martinez, M. A.; Dyballa, M.; Hunger, M.; Traa, Y.; Hirth, T.; Klemm, E. Deactivation Behavior of Alkali-Metal Zeolites in the Dehydration of Lactic Acid to Acrylic Acid. *J. Catal.* **2015**, *329*, 413–424. https://doi.org/10.1016/j.jcat.2015.05.017.

(39) Eller, K. Process and Catalysts for the Preparation of Alkoxycarboxylate Esters from Hydroxycarboxylate Esters and Alcohols. US 5,453,534, 1995.

(40) Yan, B.; Tao, L.-Z.; Liang, Y.; Xu, B.-Q. Sustainable Production of Acrylic Acid: Alkali-Ion Exchanged Beta Zeolite for Gas-Phase Dehydration of Lactic Acid. *ChemSusChem* **2014**, *7* (6), 1568–1578. https://doi.org/10.1002/cssc.201400134.

(41) Ward, J. W. Spectroscopic Study of the Surface of Zeolite Y: The Adsorption of Pyridine. *J. Colloid Interface Sci.* **1968**, *28* (2), 269–278. https://doi.org/10.1016/0021-9797(68)90130-6.

(42) Barthomeuf, D. Conjugate Acid-Base Pairs in Zeolites. *J. Phys. Chem.* **1984**, *88* (1), 42–45. https://doi.org/0.1021/j150645a010.

(43) Kladnig, W. Surface Acidity of Cation Exchanged Y-Zeolites. *J. Phys. Chem.* **1976**, *80* (3), 262–269. https://doi.org/10.1021/j100544a012.

(44) Cassanas, G.; Morssli, M.; Fabregue, E.; Bardet, L. Vibrational Spectra of Lactic Acid and Lactates. *J. Raman Spectrosc.* **1991**, *22* (7), 409–413. https://doi.org/10.1002/jrs.1250220709.

(45) Murphy, B. M.; Letterio, M. P.; Xu, B. Selectivity Control in the Catalytic Dehydration of Methyl Lactate: The Effect of Pyridine. *ACS Catal.* **2016**, *6* (8), 5117–5131. https://doi.org/10.1021/acscatal.6b00723.

(46) Murphy, B. M.; Letterio, M. P.; Xu, B. Catalyst Deactivation in Pyridine-Assisted Selective Dehydration of Methyl Lactate on NaY. *ACS Catal.* **2017**, *7* (3), 1912–1930. https://doi.org/10.1021/acscatal.6b03166.

(47) Murphy, B. M.; Letterio, M. P.; Xu, B. Catalytic Dehydration of Methyl Lactate: Reaction Mechanism and Selectivity Control. *J. Catal.* **2016**, *339*, 21–30. https://doi.org/10.1016/j.jcat.2016.03.026.

(48) Murphy, B. M.; Mou, T.; Wang, B.; Xu, B. The Effect of Cofed Species on the Kinetics of Catalytic Methyl Lactate Dehydration on NaY. *ACS Catal.* **2018**, *8* (10), 9066–9078. https://doi.org/10.1021/acscatal.8b02125.

(49) Sad, M. E.; Gonzalez Pena, L. F.; Padro, C. L.; Apesteguia, C. R. Selective Synthesis of Acetaldehyde from Lactic Acid on Acid Zeolites. *Catal. Today* **2018**, *302*, 203–209. https://doi.org/10.1016/j.cattod.2017.03.024.

(50) Inkinen, S.; Hakkarainen, M.; Albertsson, A.-C.; Sodergard, A. From Lactic Acid to Poly(Lactic Acid) (PLA): Characterization and Analysis of PLA and Its Precursors. *Biomacromolecules* **2011**, *12* (3), 523–532. https://doi.org/10.1021/bm101302t.

(51) McNeill, I. C.; Leiper, H. A. Degradation Studies of Some Polyesters and Polycarbonates—2. Polylactide: Degradation under Isothermal Conditions, Thermal Degradation Mechanism and Photolysis of the Polymer. *Polym. Degrad. Stab.* **1985**, *11* (4), 309–326. https://doi.org/10.1016/0141-3910(85)90035-7.

SYNOPSIS

Aiming the process of bio-based production of acrylate monomers, namely methyl acrylate, potassium modified ZSM-5 zeolites were studied for the process of gas-phase methyl lactate conversion.

TOC

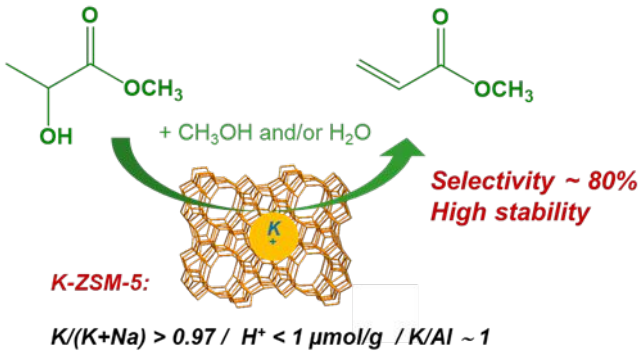

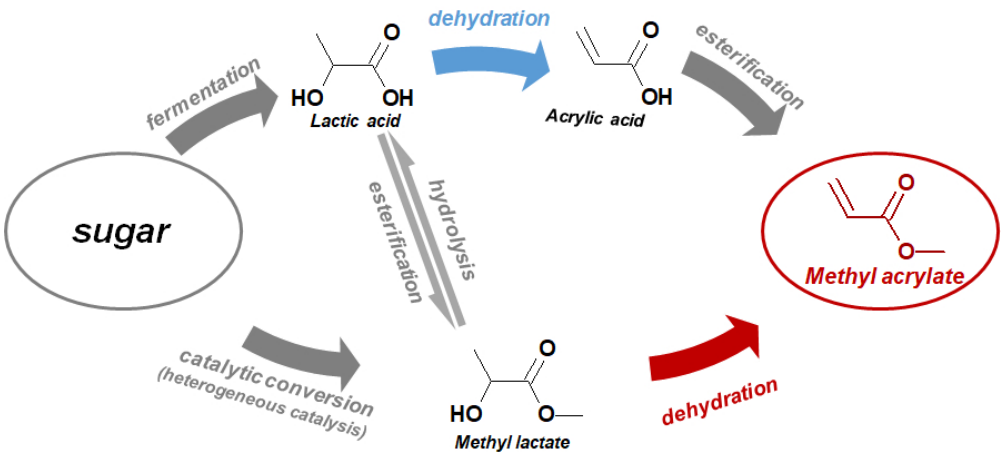

Scheme 1. Overview of the different processes for production of bio-acrylic acid and esters from sugars via lactic intermediates. The blue colored route indicates the most studied pathway in literature; the red colored route indicates the pathway of this work.

158x73mm (144 x 144 DPI)

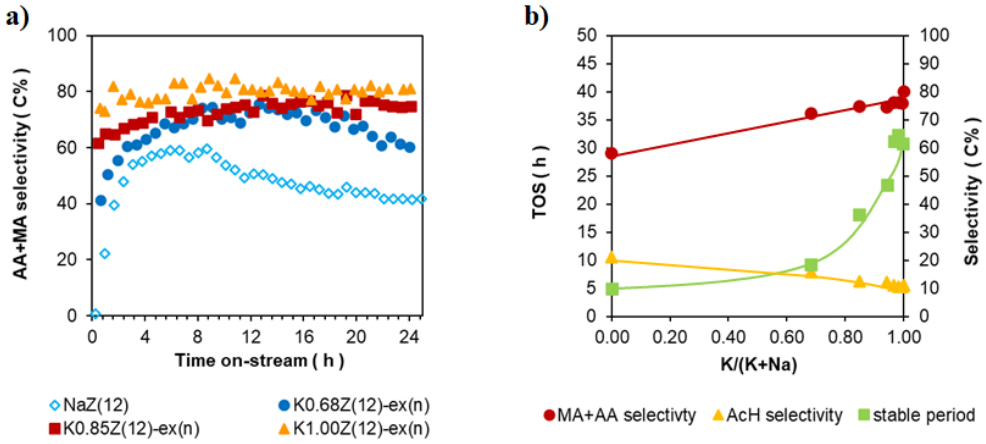

Figure 1. (a) Time-on-stream behavior (TOS), and (b) the impact of K exchange degree in ZSM-5 on stability and selectivity, tested in ML conversion in following conditions: 340°C, 35 wt.% ML in MeOH, and 5.6 mol.% of ML in total gas stream (0.5 h^{-1} liquid hourly space velocity - LHSV). The lines are guides to the eye.

144x65mm (144 x 144 DPI)

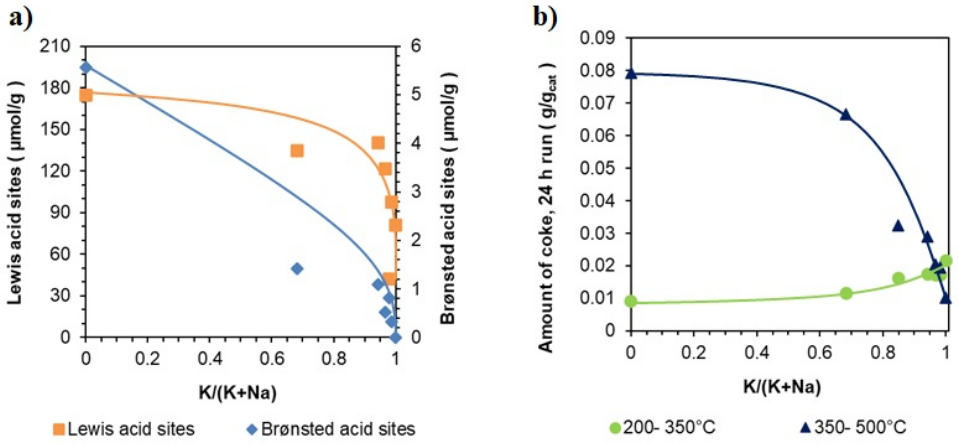

Figure 2. Amount of Lewis and Brønsted acid sites (a) and amount of coke accumulated during 24h runs (b) vs. potassium content. The lines are guides to the eye.

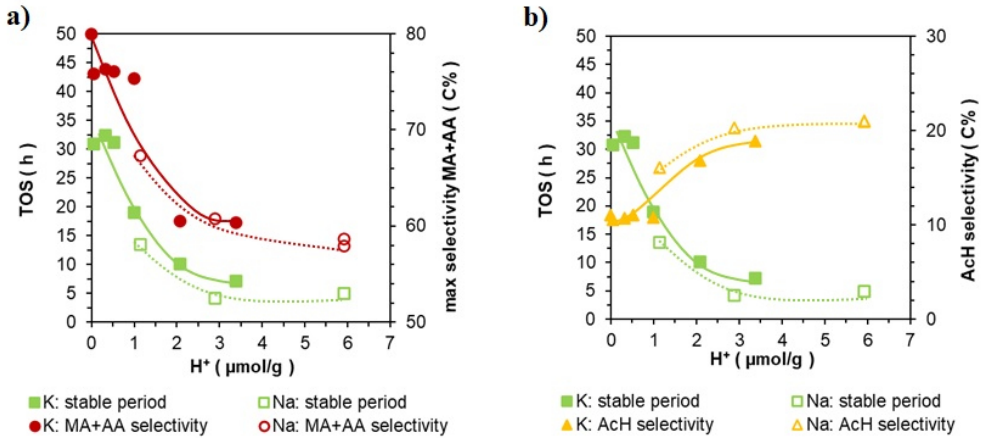

Figure 3. Effect of residual Brønsted acid on stability and acrylates selectivity (a) and acetaldehyde selectivity (b). Reaction conditions: 340°C, 35 wt.% ML in MeOH, 5.6 mol.% of ML in total gas stream corresponding to 0.5 h^{-1} LHSV. The lines are guides to the eye

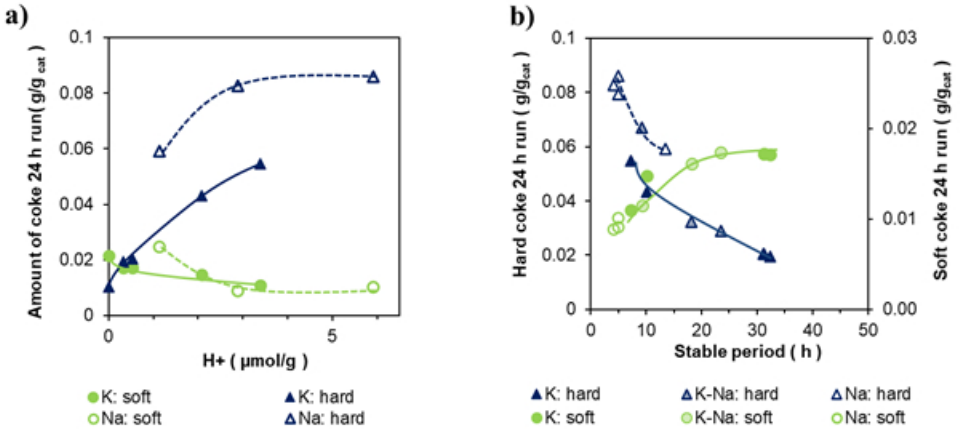

Figure 4. Coke content (a) of the Na- (open symbols) and K-ZSM-5(12) materials (closed symbols) with different content of Brønsted acid sites in ML conversion; (b) relationship between hard and soft coke content on the spent catalysts and the catalytic stability on stream for 3 series of catalysts with only Na, only K and mixed Na-K with different H^+-content (coke content analyzed after 24h run) The lines are guides to the eye

110x50mm (144 x 144 DPI)

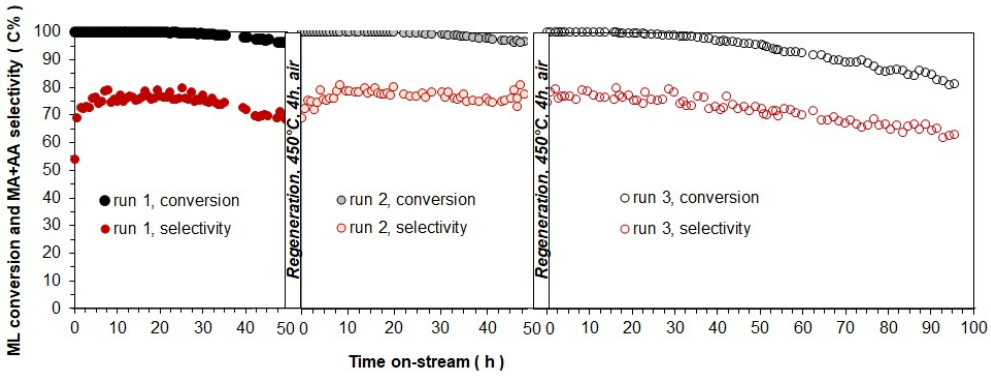

Figure 5. Time-on-stream (TOS) behavior of proton-free K-ZSM-5 catalyst with 2 regeneration steps (calcination in air at 450°C, 4 h) after 50h run (reaction conditions: 340°C, liquid feedstock: 35 wt.% ML/MeOH, 5.6 mol.% of ML in total gas stream). Fig. S9 shows a full overlap of run 1 and run 3 (fresh catalyst and catalyst after 2 regeneration cycles)

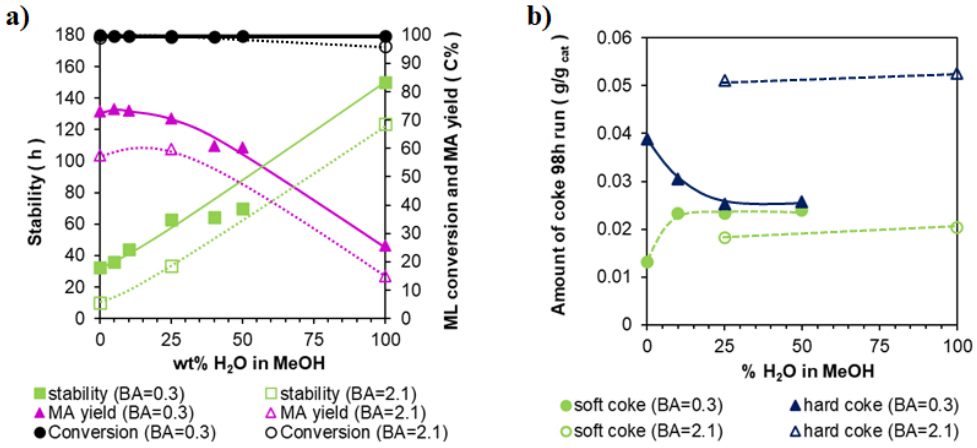

Figure 6. Water effect on the catalytic performance (a) and coke content (b) of K-ZSM-5 with low (0.3 μmol g^{-1}) and high (2.1 μmol g^{-1}) Brønsted acidity (BA) content in ML conversion. C conditions: 340°C, liquid feedstock: 35 wt.% ML / X wt% H2O in MeOH, 5.6 mol.% of ML in total gas stream. The lines are guides to the eye.

143x65mm (144 x 144 DPI)

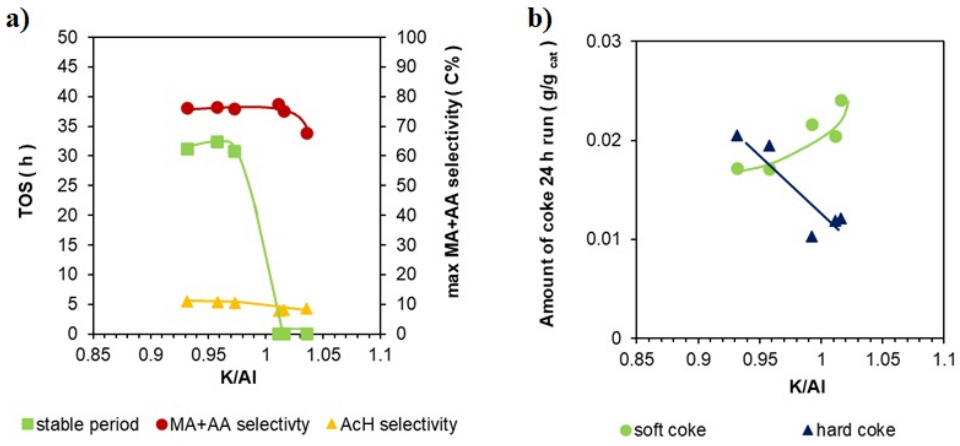

Figure 7. Catalytic performance (a) and coke content (b) of the K-rich K-ZSM-5(12) materials with varying K/Al ratio (K/(K+Na) > 0.97) but similar Brønsted acidity (<1 μmol g^{-1}) in ML conversion. Reaction conditions: 340°C, 35 wt.% ML in MeOH, 5.6 mol.% of ML in total gas stream (0.5 h^{-1} LHSV)

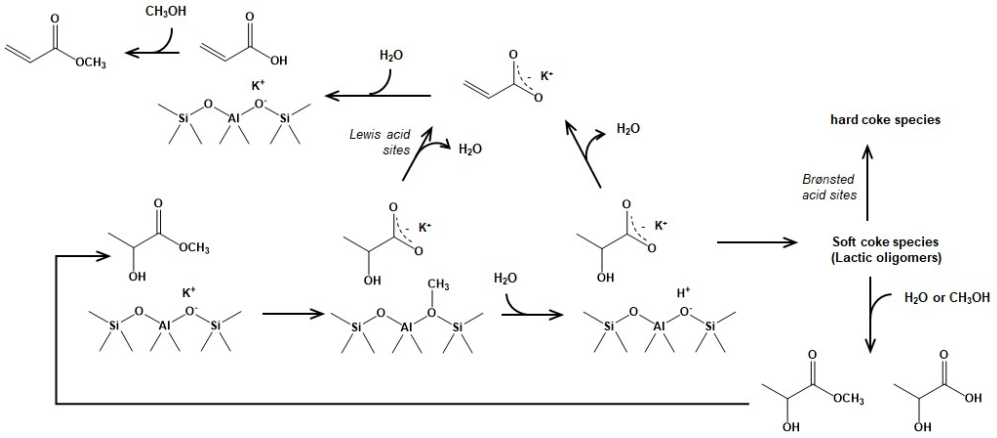

Scheme 2. Tentative scheme of the process including formation of acrylates, coke formation, recuperation of the substrate through partial decomposition of soft coke

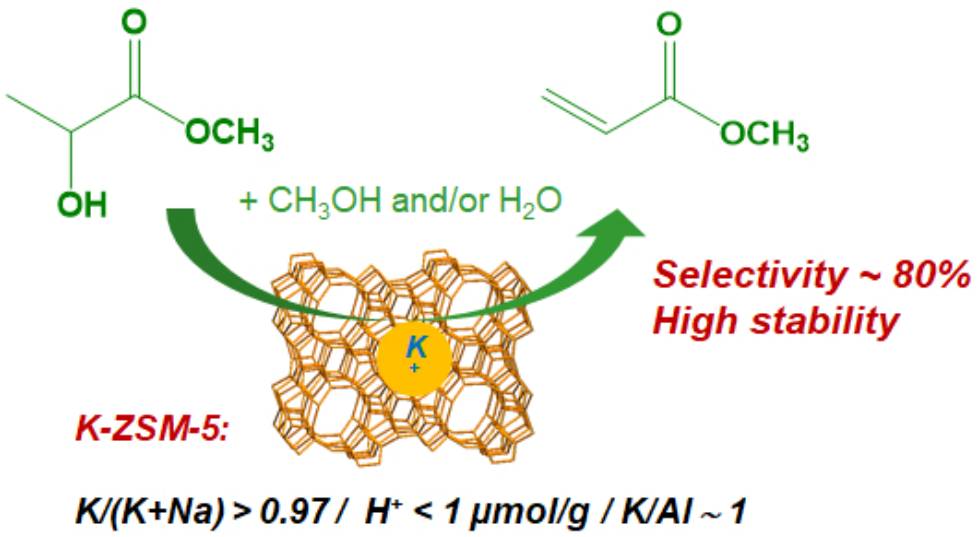

Table of contents artwork

95x52mm (144 x 144 DPI)